A kinetic analysis on non-isothermal glass–crystal transformation in $Ge_{1-x}Sn_xSe_{2.5}$ ($0 \leq x \leq 0.5$) glasses

2009 J. Phys.: Condens. Matter 21 335102

(http://iopscience.iop.org/0953-8984/21/33/335102)

J. Phys.: Condens. Matter **21** (2009) 335102 (8pp) doi:10.1088/0953-8984/21/33/335102

A kinetic analysis on non-isothermal glass–crystal transformation in $Ge_{1-x}Sn_xSe_{2.5}$ ($0 \leqslant x \leqslant 0.5$) glasses

Deepika, K S Rathore and N S Saxena

Semi-conductor and Polymer Science Laboratory, 5-6, Vigyan Bhawan, University of Rajasthan, Jaipur-302004, India

E-mail: deepika.spsl@gmail.com and n_s_saxena@rediffmail.com

Received 15 January 2009, in final form 5 June 2009
Published 8 July 2009
Online at stacks.iop.org/JPhysCM/21/335102

Abstract

Differential scanning calorimetry (DSC) has been employed at five different heating rates to investigate the glass–crystal transformation in $Ge_{1-x}Sn_xSe_{2.5}$ ($0 \leqslant x \leqslant 0.5$) glasses under non-isothermal conditions. From the dependence of glass transition temperature on the heating rate 'α', the activation energy of glass transition, E_t, has been calculated on the basis of the Kissinger model. Results indicate that T_g and E_t attain their minimum values at 0.3 at. wt% of Sn. The crystallization process has been investigated using Kissinger, Matusita, Augis and Bennett, and Gao and Wang models. Various kinetic parameters such as activation energy of crystallization, E_c, Avrami exponent (n), dimensionality of growth (m), frequency factor (K_o) and crystallization rate factor (K) have been calculated for a better understanding of the growth mechanism. The obtained kinetic parameters indicate that stability of glassy samples decreases upto 0.3 at. wt% of Sn and increases on further addition of Sn.

1. Introduction

Chalcogenide glasses containing S or Se or Te constitute a rich family of vitreous semiconductors. There has been an intense research activity based on these glasses because of their technological applications [1–3]. The last decade has produced strong theoretical and practical interest in the study of glass–crystal transformations. Various thermal analysis techniques have been developed to study the phase transformations of glasses. Differential scanning calorimetry (DSC) is one such technique, which is used for quantitative measurement of different kinetic parameters. Non-isothermal scanning in differential scanning calorimetry (DSC) has been widely used in the investigations of glass transition and crystallization kinetics of glasses [4–6]. There are a variety of theoretical models proposed to explain the kinetics of phase transformations in glasses.

The present paper deals with the study of glass–crystal transformation in $Ge_{1-x}Sn_xSe_{2.5}$ ($0 \leqslant x \leqslant 0.5$) glasses. Evidence of layer-like clusters as the dominant feature in the structure of melt-quenched $GeSe_2$ glass has been well established [7–14]. When this material is alloyed with second group IV element (e.g. Sn), the substitution of some Ge atoms by Sn atoms causes variation in the physical property and stability of the primary amorphous compound [15]. Studies [16, 17] have already been carried out on the $Ge_{1-x}Sn_xSe_2$ ($0 \leqslant x \leqslant 0.7$) system with emphasis on the effect of tin on the tendency for the system to phase separate into the constituent $GeSe_2$ and $SnSe_2$ binary components using Raman scattering and Mössbauer spectroscopy. Authors [18–21] studying this system have reported that there is non-monotonic behaviour with increasing Sn concentration in several measured quantities such as the index of refraction and optical band gap.

The problem with using $Ge_{1-x}Sn_xSe_2$ is the natural tendency for glass with this stoichiometric pseudo-binary composition to undergo phase separation during quenching. As a result, it is difficult to prepare completely homogeneous samples.

In the present study, $Ge_{1-x}Sn_xSe_{2.5}$ ($0 \leqslant x \leqslant 0.5$) glassy states were selected to minimize the effects mentioned above. By setting the composition on the selenium rich side, i.e. $Ge_{1-x}Sn_xSe_{2.5}$ instead of $Ge_{1-x}Sn_xSe_2$, the natural tendency for phase separation and crystallization can be reduced [22]. The main focus of the present work is to probe the details of the tin substitution process over a broad

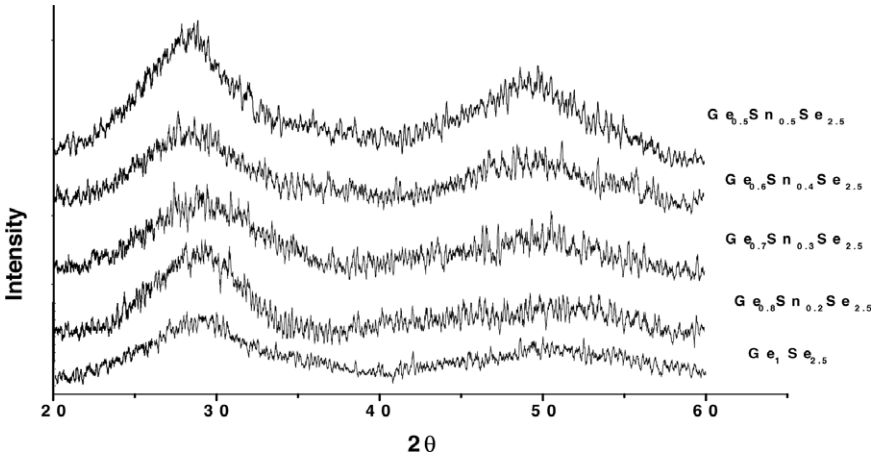

Figure 1. XRD patterns of the $Ge_{1-x}Sn_xSe_{2.5}$ ($0 \leqslant x \leqslant 0.5$) compositions.

composition range in Ge–Se glasses to better understand the glass–crystal transformation and hence, the factors affecting phase separation.

2. Experimental details

The glassy alloys of the system with x values between 0 and 0.5 have been prepared by the conventional melt quenching technique. High purity (99.999%) Ge, Sn and Se in appropriate atomic weight percentage (at. wt%) proportions were weighed into a quartz ampoule and sealed at a vacuum of 10^{-5} Torr. The ampoules were then heated at 900 °C for about 15 h with continuous rotation to facilitate the homogenization of the sample. The molten sample was rapidly quenched in ice-cooled water to produce a glassy state. The ingot of the so-produced glassy sample was taken out of the ampoule by breaking the ampoule and then grinded gently in a mortar and pestle to obtain a powder form.

The amorphous nature of the alloys was ascertained through an x-ray diffraction (XRD) pattern of the samples using Bragg–Brentano geometry on a Panalytical X'pert Pro diffractometer in a 2θ range of 20°–60° with a Cu Kα radiation source ($\lambda = 1.5406$ Å). The x-ray tube was operated at 45 kV and 40 mA.

The thermal behaviour of the samples has been investigated using a Rigaku DSC 8230. DSC runs have been taken at five different heating rates, i.e. 2, 4, 6, 8 and 10 K min^{-1} on accurately weighed samples taken in aluminium pans under non-isothermal conditions. The temperature range covered in the DSC was from room temperature (300 K) to 773 K.

3. Result and discussion

3.1. Structural and thermal analysis

Figure 1 shows the XRD diffractograms of the $Ge_{1-x}Sn_xSe_{2.5}$ ($0 \leqslant x \leqslant 0.5$) compositions at room temperature (293 K). The general features of these diffractograms emphasize the glassy nature of the so-prepared chalcogenide compositions. All the five samples of glasses ($Ge_{1-x}Sn_xSe_{2.5}$ ($0 \leqslant x \leqslant 0.5$)) show a big halo in 25°–35° of 2θ values, which is a signature of the polymeric nature of these glasses containing selenium and is also indicative of the fact that the material possesses only short range order.

The big halo is caused by broadening of diffraction peaks due to partially crystalline domains of the polymer network. Another halo, which is not as big as the first one, is obtained for a 2θ angle ranging between 45° and 55° for the samples containing Sn contents ($x \geqslant 0.3$), since addition of Sn in concentration $x \geqslant 0.3$ brings the crystalline nature to the sample, as also observed in the DSC thermogram.

The phase transformations of the samples have been observed through DSC at five different heating rates, i.e. 2, 4, 6, 8 and 10 K min^{-1} under non-isothermal conditions. Figure 2 shows the DSC thermogram of $Ge_{1-x}Sn_xSe_{2.5}$ ($0 \leqslant x \leqslant 0.5$) glassy samples at a heating rate of 6 K min^{-1}.

When the sample is heated at a constant heating rate in a DSC experiment, the glass undergoes structural changes and eventually crystallizes. In addition to the large exothermal crystallization peak, the DSC trace shows an endothermic region before crystallization occurs and this is denoted as the glass transition region. This glass transition is a kinetic phenomenon and is mainly characterized by a jump in the specific heat (C_p) value with temperature. The DSC traces of all the samples except $x = 0.3$ at. wt% Sn composition, show single glass transition and crystallization, hence, they confirm the homogeneity of the samples. The sample $Ge_{0.7}Sn_{0.3}Se_{2.5}$ glassy alloy depicts a single glass transition temperature and double crystallization with two peaks corresponding to two separate phases. These two peaks become dominant for heating rates higher than 2 K min^{-1}. Figure 3 shows the DSC thermograms of the $Ge_{0.7}Sn_{0.3}Se_{2.5}$ glassy alloy at different heating rates. For the identification of the phases, the initial glassy samples were annealed at 563 and 703 K for 2 h, which lies before the primary and secondary crystallization respectively. The annealed samples were then subjected to XRD. Figure 4 shows the XRD pattern of the annealed samples.

The XRD study reveals that $Ge_{0.7}Sn_{0.3}Se_{2.5}$ glassy alloy crystallizes into $GeSe_2$ and SnSe phases. The XRD pattern

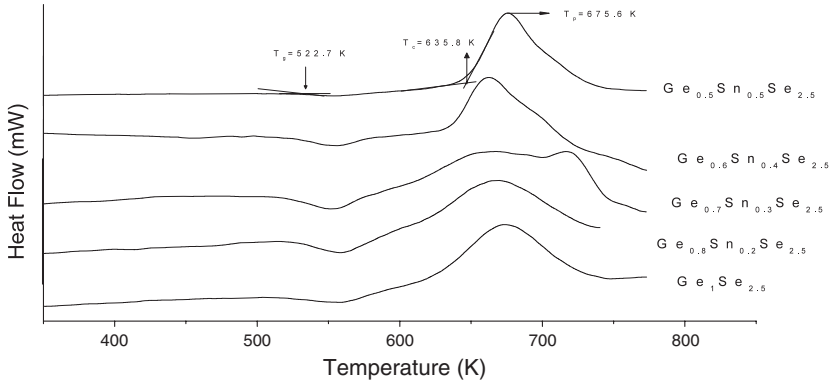

Figure 2. DSC thermogram of $Ge_{1-x}Sn_xSe_{2.5}$ ($0 \leqslant x \leqslant 0.5$) glassy samples at a heating rate of 6 K min^{-1}.

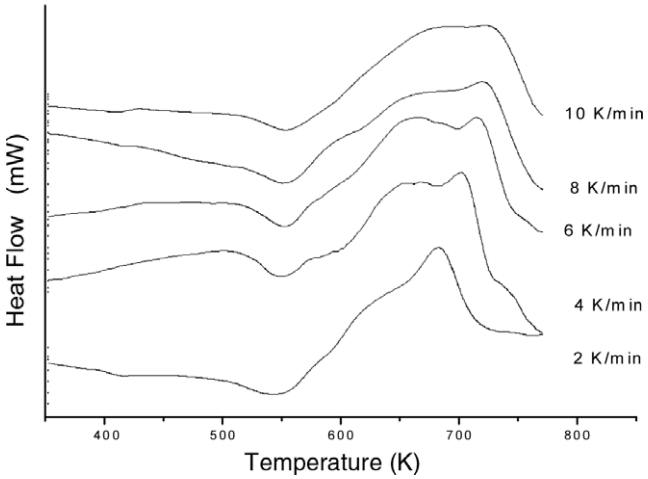

Figure 3. DSC thermograms of the $Ge_{0.7}Sn_{0.3}Se_{2.5}$ glassy alloy at different heating rates.

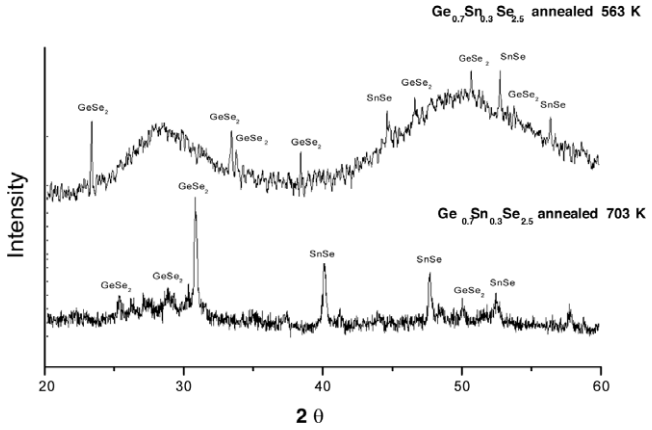

Figure 4. XRD patterns of $Ge_{0.7}Sn_{0.3}Se_{2.5}$ glassy alloy annealed at 563 and 703 K.

Table 1. Characteristic temperatures and T_c–T_g values of all the samples at a heating rate of 6 K min^{-1}.

Sample	T_g (K)	T_c (K)	T_p (K)	T_c–T_g (K)
$Ge_1Se_{2.5}$	513.1	588.9	672.9	75.8
$Ge_{0.8}Sn_{0.2}Se_{2.5}$	519.9	586.6	667.4	66.7
$Ge_{0.7}Sn_{0.3}Se_{2.5}$	515.1	579.8	668.1, 716.6	64.7
$Ge_{0.6}Sn_{0.4}Se_{2.5}$	521.0	633.4	663.0	112.4
$Ge_{0.5}Sn_{0.5}Se_{2.5}$	522.7	635.8	675.6	113.1

also show that the $GeSe_2$ phase is the dominant phase. The $GeSe_2$ phase is found to crystallize in the monoclinic structure with a unit cell defined by $a = 7.016$ Å, $b = 16.79$ Å and $c = 11.83$ Å while the SnSe phase crystallizes in the orthorhombic structure with unit cell $a = 4.310$ Å, $b = 11.70$ Å and $c = 4.318$ Å. Figure 5 shows the DSC thermogram of annealed $Ge_{0.7}Sn_{0.3}Se_{2.5}$ glassy alloys at a heating rate of 6 K min^{-1}.

DSC thermograms of a sample annealed at 563 K again show two phases with a weak primary crystallization, but as the annealing temperature is increased to 703 K, the second phase almost disappears, while the first phase remains at the same position and shows strong crystallization.

The DSC thermograms of all the samples (figure 2) show that, glass transition temperature, T_g, shifts towards a higher temperature with Sn composition for $x = 0.2$ but shows a decrease for $x = 0.3$ and on further addition of Sn upto $x = 0.5$, the T_g of the sample again increases (table 1). The decrease in T_g can be explained on the basis of the structure of the $Ge_{1-x}Sn_xSe_{2.5}$ glassy system. The structure of $GeSe_2$ in its glassy state is built up of $Ge(Se_4)_{1/2}$ tetrahedra, which form corner-sharing chains cross-linked by edge-sharing bitetrahedra. This structure forms fragments of these layers which form randomly oriented clusters terminated in the direction of the crosslinking by Se–Se bonds. The widths of these cluster varies from an average of ten chains in $GeSe_2$ to only two chains in $Ge_{1-x}Sn_xSe_2$ with $x > 0.3$. These clusters are slightly Se-rich, so that the stoichiometry must be maintained by additional units in which Ge–Ge bonds occur. In the ternary compounds Sn goes substitutionally into Ge sites preferentially occupying the sites at the edges of the clusters [15]. At $x = 0.3$, all the edge sites are fulfilled which reduces the size of the cluster within the glass, leading to a decrease in glass transition temperature. Fulfilment of all edge sites also leads to segregation of Sn atoms which results in the occurrence of two phases in the system (as shown in figure 3). The further addition of Sn upto $x = 0.5$ at. wt% results in an increase in glass transition and crystallization temperature, T_c. Initially in the $GeSe_2$ system, only Ge–Se and Se–Se bonds are present in the system. When Sn is added at the cost of

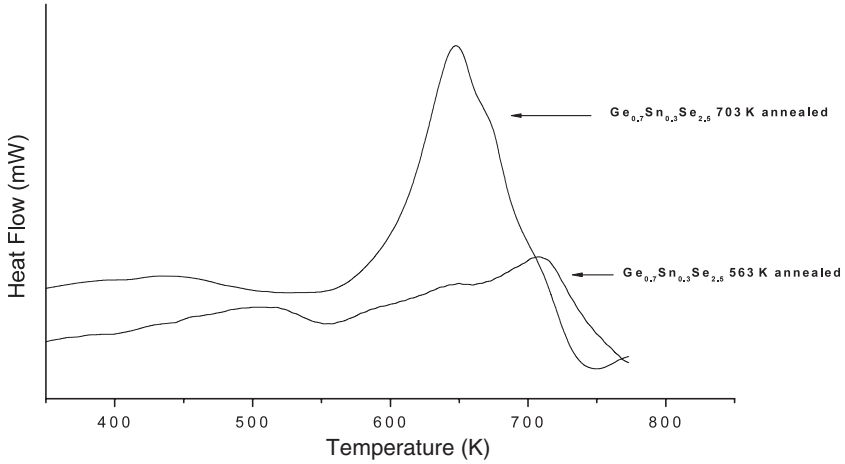

Figure 5. DSC thermograms of $Ge_{0.7}Sn_{0.3}Se_{2.5}$ glassy alloy annealed at different temperatures.

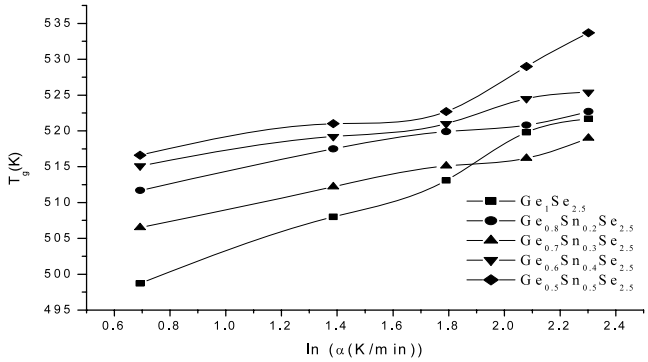

Figure 6. Plots of T_g versus $\ln(\alpha)$ for the $Ge_{1-x}Sn_xSe_{2.5}$ ($0 \leqslant x \leqslant 0.5$) glassy system.

Ge, Sn–Se bond formation takes place at the cost of Ge–Se bonds. On further addition of Sn (beyond $x = 0.3$ at. wt%) formation of Sn–Sn bonds also takes place along with Sn–Se bonds, which results in a decrease of Se–Se bonds, hence, a more ordered and rigid structure is formed. Therefore, T_g and T_c increase on addition of Sn beyond $x = 0.3$ at. wt%. The characteristic temperature T_g, T_c and peak crystallization temperature (T_p) are obtained from the DSC thermograms. T_g and T_c are extracted by extrapolation of transition elbows of endothermic and exothermic regions respectively.

Table 1 lists the characteristic temperatures and T_c–T_g values of all the samples at a heating rate of 6 K min^{-1}. Table 1 shows that the $Ge_{0.7}Sn_{0.3}Se_{2.5}$ sample is least stable among the whole series.

From table 1, it is observed that there is a slight decrease in T_g for a $Ge_{0.7}Sn_{0.3}Se_{2.5}$ glassy system, the reason for which has already been discussed above. The least value of T_c–T_g at $x = 0.3$ composition of Sn also infers that this sample ($Ge_{0.7}Sn_{0.3}Se_{2.5}$) is least stable as compared to others as glass transition as well as crystallization occurs earlier in this sample. Besides, the glass with this said composition of Sn shows a greater tendency of phase separation during crystallization as is evident from figure 2.

Table 2. The values of A, B and activation energy of glass transition (E_t) for $Ge_{1-x}Sn_xSe_{2.5}$ ($0 \leqslant x \leqslant 0.5$) glassy alloys.

			Activation energy of glass transition (E_t) (kJ mol^{-1})
Composition	A (K)	B (min)	Kissinger model
$Ge_1Se_{2.5}$	488.1	14.62 ± 0.84	155.16 ± 1.12
$Ge_{0.8}Sn_{0.2}Se_{2.5}$	507.5	6.62 ± 0.51	270.13 ± 0.55
$Ge_{0.7}Sn_{0.3}Se_{2.5}$	501.5	7.43 ± 0.44	318.96 ± 1.17
$Ge_{0.6}Sn_{0.4}Se_{2.5}$	510.3	6.49 ± 0.55	317.17 ± 0.22
$Ge_{0.5}Sn_{0.5}Se_{2.5}$	512.0	10.0 ± 0.08	309.07 ± 0.58

3.2. Kinetics of phase transformations

Glass transition region

The glass transition region has been studied in terms of the glass transition temperature with composition and heating rate. In addition to this, the activation energy of the glass transition (E_t) has also been evaluated and the composition dependence of E_t has been investigated.

The dependence of T_g on heating rate (α) can be discussed on the basis of two approaches. The first approach is the empirical relation suggested by Lasocka [23], which has the form:

$$T_g = A + B \ln \alpha \tag{1}$$

where A and B are constants for a given glass composition. The value of A indicates the glass transition temperature for the heating rate of 1 K min^{-1}, while the value of B determines the time response of configurational changes within the glass transition region to the heating rate. Figure 6 depicts the plots of T_g versus $\ln(\alpha)$ for the investigated $Ge_{1-x}Sn_xSe_{2.5}$ ($0 \leqslant x \leqslant 0.5$) glassy system. It is found that this equation holds good for our samples. The values of A and B for all the samples are listed in table 2.

The second approach that shows the dependence of T_g on heating rate is known as the Kissinger formulation [24]. This equation is employed for the evaluation of the activation energy of glass transition, E_t. In spite of the fact that the Kissinger equation is basically for the determination of activation energy of crystallization process, it has been frequently used for the

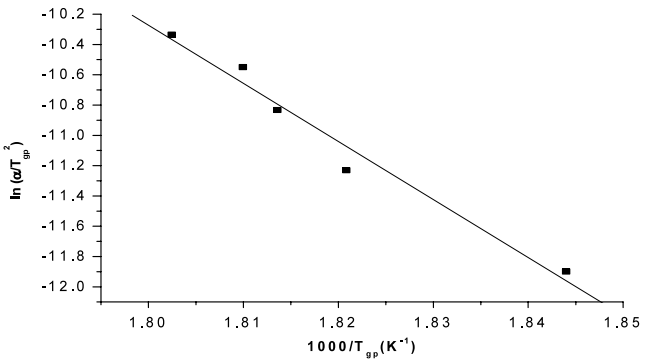

Figure 7. Plot of $\ln(\alpha/T_{gp}^2)$ against $1000/T_{gp}$ for $Ge_{0.7}Sn_{0.3}Se_{2.5}$ glassy sample.

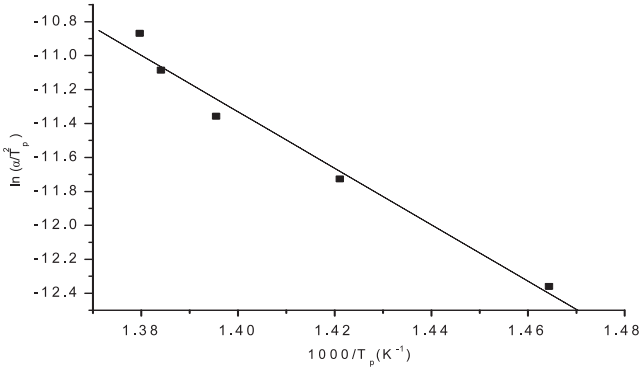

Figure 8. Plot between $\ln(\alpha/T_p^2)$ and $1000/T_p$ for the $Ge_{0.7}Sn_{0.3}Se_{2.5}$ glassy sample.

determination of the activation energy of glass transition using the peak glass transition temperatures. In non-isothermal conditions, the sample is heated at constant heating rate, and the evolved heat is recorded as a function of temperature. If the reaction proceeds at a rate varying with temperature, the position of the peak varies with the heating rate. This temperature shift, in turn, can be used to calculate the kinetic parameters of crystallization [25]. If the shift in the glass transition peak with heating rate is similar to peak shifts in the crystallization region, then this equation can be used for the determination of the activation energy of glass transition. This condition is satisfied in measurements mentioned in this study. The Kissinger equation relating the peak glass transition temperature with heating rate is given by:

$$\ln(\alpha/T_{gp}^2) = -E_t/RT_{gp} + \text{const} \tag{2}$$

where T_{gp} is the peak glass transition temperature and R is the gas constant. A graph is plotted between $\ln(\alpha/T_{gp}^2)$ and $1000/T_{gp}$, which yields a straight line and the slope $(-E_t/R)$ of this straight line gives the activation energy of glass transition (E_t). Figure 7 shows the plot of $\ln(\alpha/T_{gp}^2)$ against $1000/T_{gp}$ for $Ge_{0.7}Sn_{0.3}Se_{2.5}$ glassy sample as a representative case.

The values of E_t for all the compositions are also listed in table 2. From table 2, it is observed that the activation energy of the glass transition E_t increases with Sn addition upto $x = 0.3$ and decreases on further addition of Sn. Hence, one can infer that on addition of Sn beyond 0.3 at. wt%, less energy is required by the atoms to go to a more stable state.

Crystallization. Generally, the crystallization process is well characterized when the three kinetic parameters, activation energy of crystallization (E_c), Avrami exponent (n) and frequency factor (K_o) are determined. In non-isothermal crystallization, it is assumed that there is a constant heating rate in the experiment. The activation energy of crystallization, E_c, has been deduced using the following theoretical models.

Kissinger model. The activation energy for crystallization, E_c, can be obtained from the heating-rate dependence of peak temperature of crystallization, T_p, using the equation derived by Kissinger [24].

$$\ln(\alpha/T^2) = -E/RT_p + \text{const} \tag{3}$$

where T_p is the peak crystallization temperature. Figure 8 shows the relation between $\ln(\alpha/T_p^2)$ and $1000/T_p$ for the $Ge_{0.7}Sn_{0.3}Se_{2.5}$ glassy sample. The data were well fitted by a straight line.

Matusita model. The order of crystallization reaction (Avrami index, n) and the activation energy, E_c, of the amorphous–crystalline transformation can be obtained using the method suggested specifically for non-isothermal crystallization by Matusita *et al* [26]. The volume fraction of crystals (x) precipitated in a glass heated at a uniform rate (α) is related to the activation energy of crystallization through the expression

$$\ln[-\ln(1-x)] = -n\ln\alpha - 1.052mE_c/RT + \text{constant} \tag{4}$$

where m and n are constants that depend on the mechanism of the growth and the dimensionality of the crystal. If the formation of nuclei is dominant during heating at a constant rate, n is equal to $(m + 1)$. If the nuclei are predominantly formed during any previous heat treatment prior to the thermal analysis, n is equal to m [26, 27]. Plots of $\ln[-\ln(1-x)]$ versus $1000/T$ for the investigated glassy samples, measured at different heating rates, were found to be linear over most of the temperature range. The plot of $\ln[-\ln(1-x)]$ versus $1000/T$ for $Ge_{0.6}Sn_{0.4}Se_{2.5}$ glass is shown in figure 9. At high temperatures or in regions characterized by large crystallization fractions, a nonlinear behaviour was seen for all heating rates. A similar behaviour has been reported for other chalcogenide glasses [28, 29]. This nonlinear character can be attributed to the saturation of nucleation sites in the final stages of crystallization [30] or to restriction of crystal growth by small size of the particles [31]. From figure 9, the value of mE_c was calculated from the slope of the $\ln[-\ln(1-x)]$ versus $1000/T$ for all heating rates. The mE_c value was seen to be weakly dependent on the heating rate, and an average value of mE_c was therefore calculated by considering all the results obtained for the different heating rates. Figure 10 shows linear plots of $\ln[-\ln(1-x)]$ versus $\ln(\alpha)$ at three fixed temperatures for $Ge_{0.6}Sn_{0.4}Se_{2.5}$ glass. The average value of n has been calculated from the slopes of the straight lines of figure 10. The average value of n for $Ge_{0.6}Sn_{0.4}Se_{2.5}$ glass is found to be 2.08. The obtained values of Avrami exponent (n) of all the samples under investigation have been listed in table 3.

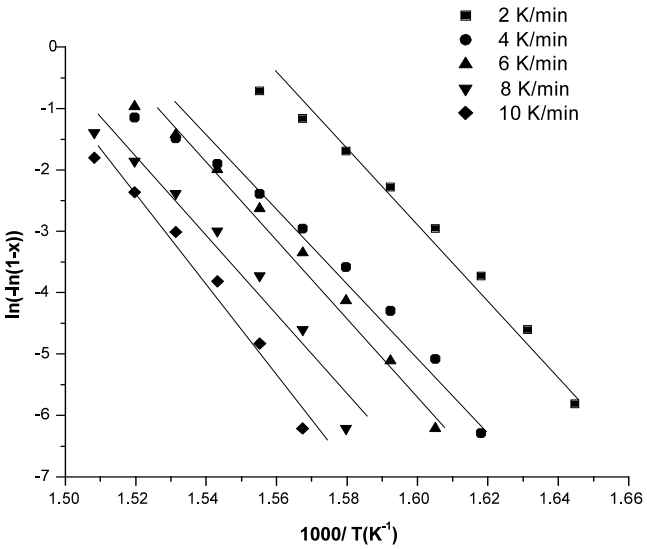

Figure 9. Plot of $\ln[-\ln(1-x)]$ versus $1000/T$ for $Ge_{0.6}Sn_{0.4}Se_{2.5}$ glass.

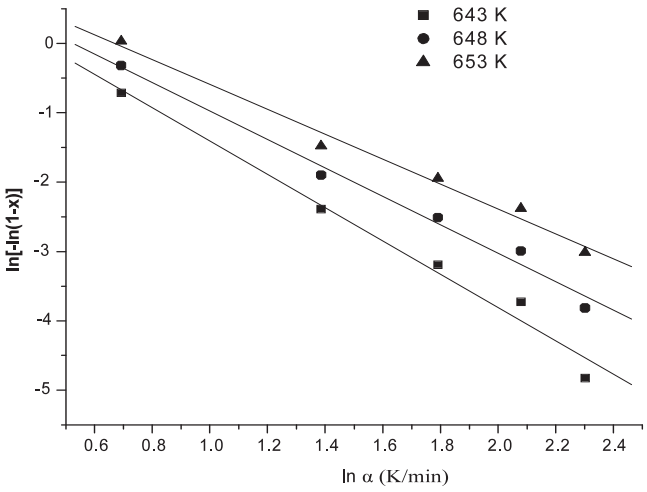

Figure 10. Plots of $\ln[-\ln(1-x)]$ versus $\ln(\alpha)$ at three fixed temperatures for $Ge_{0.6}Sn_{0.4}Se_{2.5}$ glass.

It has been found that the value of n (table 3) is not an integer. A non-integer value of n indicates that two crystallization mechanisms were working during the amorphous–crystalline transformation. But all the samples predominantly crystallize in one dimension. The obtained values of Avrami exponent (n) of all the samples under investigation have been listed in table 3.

From the value of n and the average mE_c, the activation energy for crystallization of the $Ge_{1-x}Sn_xSe_{2.5}$ ($0 \leqslant x \leqslant 0.5$) glassy alloys can be calculated.

Augis and Bennett method. The activation energy for crystallization, E_c, as well as the frequency factor (K_o), could be evaluated using the formula suggested by Augis and Bennett [32] which is given as follows:

$$\ln(\alpha/T_c) = -E_c/RT_c + \ln K_o \qquad (5)$$

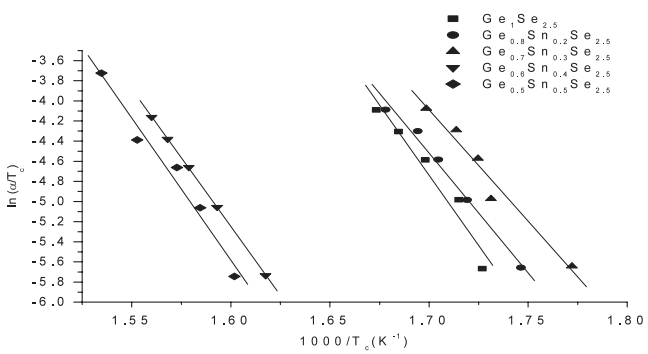

Figure 11. Plot of $\ln(\alpha/T_c)$ and $1000/T_c$ for the $Ge_{1-x}Sn_xSe_{2.5}$ ($0 \leqslant x \leqslant 0.5$) glassy system.

Table 3. Values of Avrami exponent and frequency factor for $Ge_{1-x}Sn_xSe_{2.5}$ ($0 \leqslant x \leqslant 0.5$) glassy samples.

	Avrami exponent (n)		
Sample	Matusita model	Gao and Wang model	Frequency factor (K_o)
$Ge_1Se_{2.5}$	0.96	0.75	3.64×10^{14}
$Ge_{0.8}Sn_{0.2}Se_{2.5}$	0.82	0.61	6.64×10^{15}
$Ge_{0.7}Sn_{0.3}Se_{2.5}$	0.66	0.88	3.40×10^{18}
$Ge_{0.6}Sn_{0.4}Se_{2.5}$	2.08	1.14	1.54×10^{17}
$Ge_{0.5}Sn_{0.5}Se_{2.5}$	2.46	1.38	5.34×10^{16}

where T_c is the temperature at which the crystallization just begins and K_o is the frequency factor (in s^{-1}). The relation between $\ln(\alpha/T_c)$ and $1000/T_c$ for $Ge_{1-x}Sn_xSe_{2.5}$ ($0 \leqslant x \leqslant 0.5$) glassy alloys is shown in figure 11.

The value of K_o, which is defined as the number of attempts made by the nuclei per second to overcome the energy barrier, can be evaluated from the knowledge of $\ln K_o$ from equation (5). This also provides information for the calculation of nucleation sites, present in the material for crystal growth. The value of K_o for all the samples is given in table 3. The maximum value of K_o again confirms the fact that $Ge_{0.7}Sn_{0.3}Se_{2.5}$ glass is least stable, as the number of attempts made by nuclei are highest for this glass. The number of attempts made by nuclei reduces after $x = 0.3$ at. wt% of Sn composition, suggesting an increase in the stability of glasses. Besides these, the crystallization rate factor (K) has also been evaluated with the help of the Arrhenius equation:

$$K = K_o \exp(-E_c/RT). \qquad (6)$$

The importance of the crystallization rate factor (K) is that its minimum value gives an indication of the retardation of the crystallization while its higher value diminishes the glass-forming ability [33]. The value of crystallization rate factor (K) obtained at 643 K is 0.496, 0.348, 0.413, 0.017, 0.012 for $Ge_1Se_{2.5}$, $Ge_{0.8}Sn_{0.2}Se_{2.5}$, $Ge_{0.7}Sn_{0.3}Se_{2.5}$, $Ge_{0.6}Sn_{0.4}Se_{2.5}$, $Ge_{0.5}Sn_{0.5}Se_{2.5}$ respectively. It is observed that there is a drastic decrease in the value of K after $x = 0.3$ at. wt% composition of Sn, which suggests an increase in stability of samples after $x = 0.3$ at.wt% of Sn.

Gao and Wang model. Gao and Wang [34] proposed a slightly different method to analyse DSC thermograms in terms of the

Table 4. Activation energy of crystallization (E_c) of $Ge_{1-x}Sn_xSe_{2.5}$ ($0 \leqslant x \leqslant 0.5$) glassy systems using different theoretical models.

	Activation energy of crystallization (E_c) (kJ mol^{-1})			
Composition	Kissinger model	Matusita model	Augis and Bennet model	Gao and Wang model
$Ge_1Se_{2.5}$	164.30 ± 1.29	162.71 ± 1.40	231.86 ± 1.59	229.51 ± 1.20
$Ge_{0.8}Sn_{0.2}Se_{2.5}$	150.24 ± 1.40	146.41 ± 1.63	200.40 ± 1.04	211.89 ± 1.48
$Ge_{0.7}Sn_{0.3}Se_{2.5}$	138.29 ± 1.18	145.24 ± 1.75	183.97 ± 1.20	110.36 ± 6.90
$Ge_{0.6}Sn_{0.4}Se_{2.5}$	193.17 ± 1.26	189.20 ± 1.79	227.41 ± 1.16	171.22 ± 1.38
$Ge_{0.5}Sn_{0.5}Se_{2.5}$	208.18 ± 1.72	207.13 ± 1.90	234.67 ± 1.67	175.10 ± 1.64

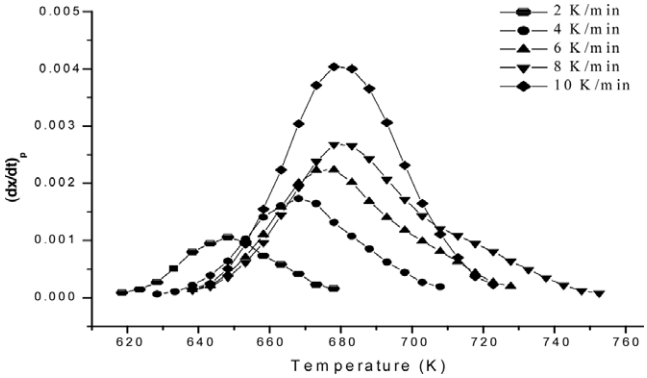

Figure 12. Plot of $(dx/dt)_p$ against temperature (T) at different heating rates for $Ge_{0.5}Sn_{0.5}Se_{2.5}$ glass.

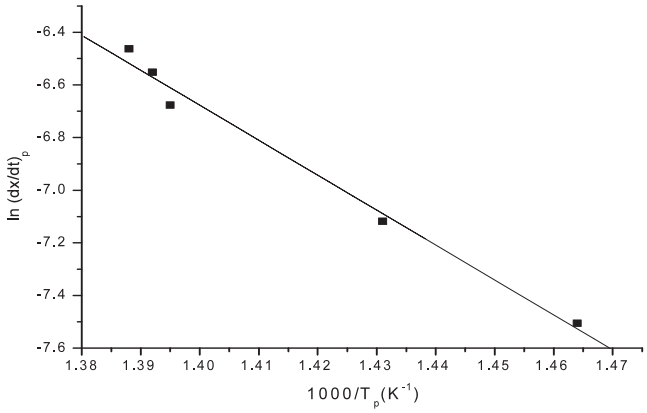

Figure 13. Plot of $\ln(dx/dt)_p$ versus $1000/T_p$ for $Ge_{0.7}Sn_{0.3}Se_{2.5}$ glass.

activation energy E_c, the dimensionality m, the rate constant in atomic diffusion, the microstructure of amorphous alloy K, the frequency factor K_o etc, during the crystallization process. This theory is based on the same fundamental assumptions imposed on the Johnson–Mehl–Avrami (JMA) transformation equation. It assumes that the nucleation is randomly distributed and that the growth rate of the new phase depends on the temperature but not on time. The theory provides the relationship between the maximum crystallization rate and the peak crystallization temperature, which is given by:

$$\ln(dx/dt)_p = -E/RT_p + \text{const} \tag{7}$$

where $(dx/dt)_p$ is the rate of volume fraction crystallized at the peak of crystallization T_p, which is proportional to the exothermic peak height. Figure 12 shows the plot of $(dx/dt)_p$ against temperature (T) at different heating rates for $Ge_{0.5}Sn_{0.5}Se_{2.5}$ glass.

It is clear from figure 12 that the peak height increases and shifts towards higher temperature values with the increase in heating rate. This is due to the fact that as the heating rate is increased from 2 to 10 K min^{-1}, the rate of crystallization increases and crystallization shifts towards higher temperatures hence, the peak shifts towards higher temperature values. Again we can say that with this increased rate of crystallization, a greater volume fraction is crystallized in a smaller time as compared to the low heating rate, which further signifies the increased peak height with increase in heating rate in these curves.

Gao and Wang plots (plot of $\ln(dx/dt)_p$ versus $1000/T_p$) for $Ge_{0.7}Sn_{0.3}Se_{2.5}$ glass is shown in figure 13 as a representative case. These plots are fitted to straight lines and the slope of these straight lines gives the activation energy of crystallization (E_c).

The Gao and Wang method is also used to evaluate the Avrami exponent using the following relations:

$$(\alpha E_c/RT^2)K_p = 1 \tag{8}$$

$$K_p = K_o \exp(-E_c/RT_p) \tag{9}$$

$$(dx/dt)_p = 0.37nK_p. \tag{10}$$

The values of Avrami exponent (n) obtained using the above relation are shown in table 3.

It is evident from table 3 that values of Avrami exponent (n) obtained from the Gao–Wang and Matusita models differ from each other. This difference in values is due to the difference in the procedures for the calculation of n as discussed above. The values of Avrami exponent from the Gao–Wang model again confirm that glass predominantly crystallizes in one dimension (since $m = n - 1$) suggesting surface nucleation.

Table 4 lists the values of activation energy of crystallization (E_c) of $Ge_{1-x}Sn_xSe_{2.5}$ ($0 \leqslant x \leqslant 0.5$) glassy systems using different theoretical models. From table 4, it is clear that the activation energy of crystallization decreases upto $x = 0.3$ at. wt% of Sn composition and increases on further addition of Sn, therefore one can conclude that the stability of the sample decreases upto $x = 0.3$ at. wt% of Sn composition, as atoms require a small amount of energy to jump from the glassy state to the crystalline state, while on further addition of Sn, an increase in activation energy suggests stability of the samples.

From the above, we know that the activation energies of amorphous alloys calculated by means of the different theoretical models differ substantially from each other. This difference in the activation energy as calculated with the different models, even for the same sample, may be attributed to the different approximations used in the models. The Kissinger equation was basically developed for studying the variation of the peak crystallization temperature with heating rate. According to Kissinger's method, the transformation under non-isothermal conditions is represented by a first-order reaction. Moreover, the concept of nucleation and growth has not been included in the Kissinger equation. Matusita *et al* have developed a method on the basis of the fact that crystallization does not advance by an nth-order reaction but by a nucleation and growth process. They emphasized that crystallization mechanisms such as bulk crystallization (bulk nucleation followed by two-or three-dimensional growth) or surface crystallization (bulk nucleation followed by linear growth) should be taken into account for obtaining E_c. In addition to activation energy, Matusita's method provides information about the Avrami exponent and dimensionality of growth. The Augis and Bennett method is helpful in obtaining kinetic parameters such as frequency factor (K_o), rate constant (K) along with activation energy of crystallization and is therefore preferred for the calculation of the kinetics over the other models.

4. Conclusions

The phase transformation kinetics of $Ge_{1-x}Sn_xSe_{2.5}$ ($0 \leqslant x \leqslant 0.5$) glasses has been carried out using several theoretical models and the following conclusions can be made.

(1) The glassy alloys under investigation (except $x = 0.3$) show a single glass transition and crystallization region, confirming the homogeneity of the samples. Sample $Ge_{0.7}Sn_{0.3}Se_{2.5}$ shows a single glass transition and double crystallization peak corresponding to two phases.
(2) The crystalline phases ($GeSe_2$ and SnSe) developed in $Ge_{0.7}Sn_{0.3}Se_{2.5}$ glassy samples are similar when annealed at different temperatures. XRD results show that the dominant phase is the $GeSe_2$ phase, the SnSe phase was also identified.
(3) The T_c–T_g is lowest for a $Ge_{0.7}Sn_{0.3}Se_{2.5}$ glassy sample, therefore the sample is the least stable compared with other samples. The values of E_t, E_c also confirm the same fact.
(4) Besides activation energy, crystallization rate factor (K) and frequency factor (K_o) have also been determined and they suggest that glass-forming ability increases after $x = 0.3$ at. wt% composition of Sn.

References

[1] Soliman A A 2004 *Thermochim. Acta* **423** 71
[2] Vazquez J, Lopez-Alemany P L, Villares P and Jimenez-Garay R 2003 *J. Alloys Compounds* **354** 153
[3] Pattanaik A K and Srinivasan A 2005 *J. Appl. Sci.* **5** 1
[4] Maharjan N B, Bhandari D, Saxena N S, Paudyal D D and Husain M 2000 *Ind. J. Phys.* A **74** 343
[5] Malek J 1999 *J. Therm. Anal. Calorim.* **56** 763
[6] Deepika, Saraswat V K, Jain P K, Saxena N S, Sharma K, Sharma T P and Dhawan S K 2008 *AIP Proc.* **1004** 85
[7] Bridenbaugh P M, Espinosa G P, Griffiths J E, Phillips J C and Remeika J P 1979 *Phys. Rev.* B **20** 4140
[8] Griffiths J E, Espinosa G P, Phillips J C and Remeika J P 1983 *Phys. Rev.* B **28** 4444
[9] Weinstein B A, Zallen R, Slade M L and Mikkelsen J C Jr 1982 *Phys. Rev.* B **25** 781
[10] Bresser W J, Boolchand P, Suranyi P and Deneufville J P 1981 *Phys. Rev. Lett.* **46** 1689
[11] Boolchand P, Grothaus J, Bresser W J and Suranyi P 1982 *Phys. Rev.* B **25** 2975
[12] Boolchand P, Grothaus J and Phillips J C 1983 *Solid State Commun.* **48** 183
[13] Phillips J C 1981 *J. Non-Cryst. Solids* **43** 37
[14] Boolchand P and Stevens M 1984 *Phys. Rev.* B **29** 1
[15] Fayek S A and Ali M H 1995 *J. Mater. Sci.* **30** 2838
[16] Stevens M, Boolchand P and Hernandez J G 1985 *Phys. Rev.* B **31** 981
[17] Mcneil L E, Mikrut J M and Peters M J 1987 *Solid State Commun.* **62** 101
[18] Mikrut J M and Mcneil L E 1989 *J. Non-Cryst. Solids* **114** 127
[19] Islam D, Brient C E and Cappelletti R L 1990 *J. Mater. Res.* **5** 511
[20] Martin L W, Mcneil L E and Mikrut J M 1990 *Phil. Mag.* B **61** 957
[21] Islam D and Cappelletti R L 1991 *Phys. Rev.* B **44** 2516
[22] Phillips J C 1979 *J. Non-Cryst. Solids* **34** 153
[23] Lasocka M 1976 *Mater. Sci. Eng.* **23** 173
[24] Kissinger H E 1956 *J. Res. Nat. Bur. Stand.* **57** 217
[25] White K, Crane R L and Snide J A 1988 *J. Non-Cryst. Solids* **103** 210
[26] Matusita K, Konatsu T and Yokota R 1984 *J. Mater. Sci.* **19** 291
[27] Matusita K and Sakka S 1979 *Phys. Chem.* **20** 81
[28] Colemenero J and Barandiaran J M 1978 *J. Non-Cryst. Solids* **30** 263
[29] Speyer R F and Hrisbud S 1983 *Phys. Chem. Glasses* **24** 26
[30] Imran M M A, Saxena N S, Bhandari D and Husain M 2000 *Phys. Status Solidi* a **181** 357
[31] Kaur G and Komatsu T 2001 *J. Mater. Sci.* **36** 4531
[32] Augis J A and Bennett J E 1978 *J. Therm. Anal. Calor.* **13** 283
[33] Weinberg M C 1986 *J. Non-Cryst. Solids* **167** 8
[34] Gao Y Q and Wang W 1986 *J. Non-Cryst. Solids* **87** 129